ARTICLE

doi:10.1038/nature10703

Antiparallel EmrE exports drugs by exchanging between asymmetric structures

Emma A. Morrison[1]*, Gregory T. DeKoster[1]*, Supratik Dutta[1], Reza Vafabakhsh[2], Michael W. Clarkson[3], Arjun Bahl[1], Dorothee Kern[3], Taekjip Ha[2] & Katherine A. Henzler-Wildman[1]

Small multidrug resistance transporters provide an ideal system to study the minimal requirements for active transport. EmrE is one such transporter in *Escherichia coli*. It exports a broad class of polyaromatic cation substrates, thus conferring resistance to drug compounds matching this chemical description. However, a great deal of controversy has surrounded the topology of the EmrE homodimer. Here we show that asymmetric antiparallel EmrE exchanges between inward- and outward-facing states that are identical except that they have opposite orientation in the membrane. We quantitatively measure the global conformational exchange between these two states for substrate-bound EmrE in bicelles using solution NMR dynamics experiments. Förster resonance energy transfer reveals that the monomers within each dimer are antiparallel, and paramagnetic relaxation enhancement NMR experiments demonstrate differential water accessibility of the two monomers within each dimer. Our experiments reveal a 'dynamic symmetry' that reconciles the asymmetric EmrE structure with the functional symmetry of residues in the active site.

EmrE is a secondary active antiporter, driving uphill transport of each polyaromatic cation substrate against its concentration gradient by coupling it to downhill import of two protons across the inner membrane. As one of the smallest known active transporters, with only 110 amino acids and four transmembrane helices per monomer, EmrE would seem to be an ideal model system[1–3]. There is broad agreement that the minimal functional unit is a dimer[4–7], but its structure and topology remain controversial[3,8–13], perhaps because the membrane topology and oligomeric state are exquisitely sensitive to sequence alteration and environment[14–17].

EmrE is proposed to function through a single-site alternating access model[18–20], as shown in Fig. 1a. In this well-established model[21,22], transporters are inherently dynamic proteins, converting between inward- and outward-facing conformations to move substrates across a membrane barrier. To achieve coupled antiport, both substrates share a single binding site and conformational exchange only occurs when substrate (two protons or one polyaromatic cation) is bound. Thus, saturating EmrE with its polyaromatic cation substrate, tetraphenylphosphonium (TPP^+), should drive EmrE into a two-state equilibrium (Fig. 1a, b) suitable for direct observation and quantitative analysis of conformational exchange with site-specific resolution by solution NMR spectroscopy.

To take advantage of well-developed high-resolution solution NMR dynamics methods, we solubilized EmrE in isotropic bicelles, which surround the protein with a more native-like lipid environment than detergents while preserving the fast tumbling needed for solution NMR[23–25]. Several features of the ^1H–^{15}N transverse relaxation-optimized spectroscopy (TROSY) spectrum of TPP^+-bound $^2H/^{15}N$-EmrE in isotropic bicelles are worth noting (Fig. 1c). First, the chemical shift dispersion is much greater than expected for a helical bundle membrane protein. This dispersion is probably enhanced by ring currents from the bound polyaromatic substrate and the many aromatic residues in the binding site. Second, there are twice as many peaks (approximately 210 resolved peaks) as expected for a monomer of EmrE (105 non-proline residues). A solid-state NMR study of EmrE specifically labelled at Glu 14 (ref. 26) also noted such a peak doubling for this active-site residue in the TPP^+-bound state.

There are two possible explanations for this peak doubling: (1) an asymmetric dimer, as observed by cryo-electron microscopy and X-ray crystallography[4,7,27], where each monomer has a distinct structure and thus different chemical shifts or (2) exchange between two symmetric (parallel) homodimers that is slow on the NMR timescale. Naively, we might expect four sets of peaks in the case of both structural asymmetry and slow conformational exchange (Supplementary Fig. 1). However, as has been previously noted, there is a pseudo-twofold symmetry axis in EmrE, perpendicular to the membrane normal, such that reorientation of the helices in monomers A and B could effectively convert the structure of monomer A into that of monomer B and vice versa[18] (Fig. 1b). This unique model results in inward- and outward-facing states that are identical except for their orientation. Such a mechanism is only possible in an antiparallel homodimer, and no previous experimental data have directly tested this hypothesis.

EmrE is functional in isotropic bicelles

We first verified that EmrE is properly folded and functional in bicelles, because it has not been studied in this environment previously. To prepare bicelles, we purified EmrE in detergent, reconstituted it into liposomes and then added DHPC to form bicelles (see Methods). Extensive studies have confirmed that EmrE is a properly folded, functional dimer in dodecylmaltoside (DDM), and when reconstituted into liposomes[4,6,13,28–31]. The TROSY NMR spectra (Fig. 1c) of TPP^+-bound EmrE in dilauroylphosphatidylcholine/

[1]Department of Biochemistry and Molecular Biophysics, Washington University School of Medicine, St. Louis, Missouri 63110, USA. [2]Department of Physics and Howard Hughes Medical Institute, University of Illinois at Urbana-Champaign, Urbana, Illinois 61801, USA. [3]Department of Biochemistry and Howard Hughes Medical Institute, Brandeis University, Waltham, Massachusetts 02454, USA.
*These authors contributed equally to this work.

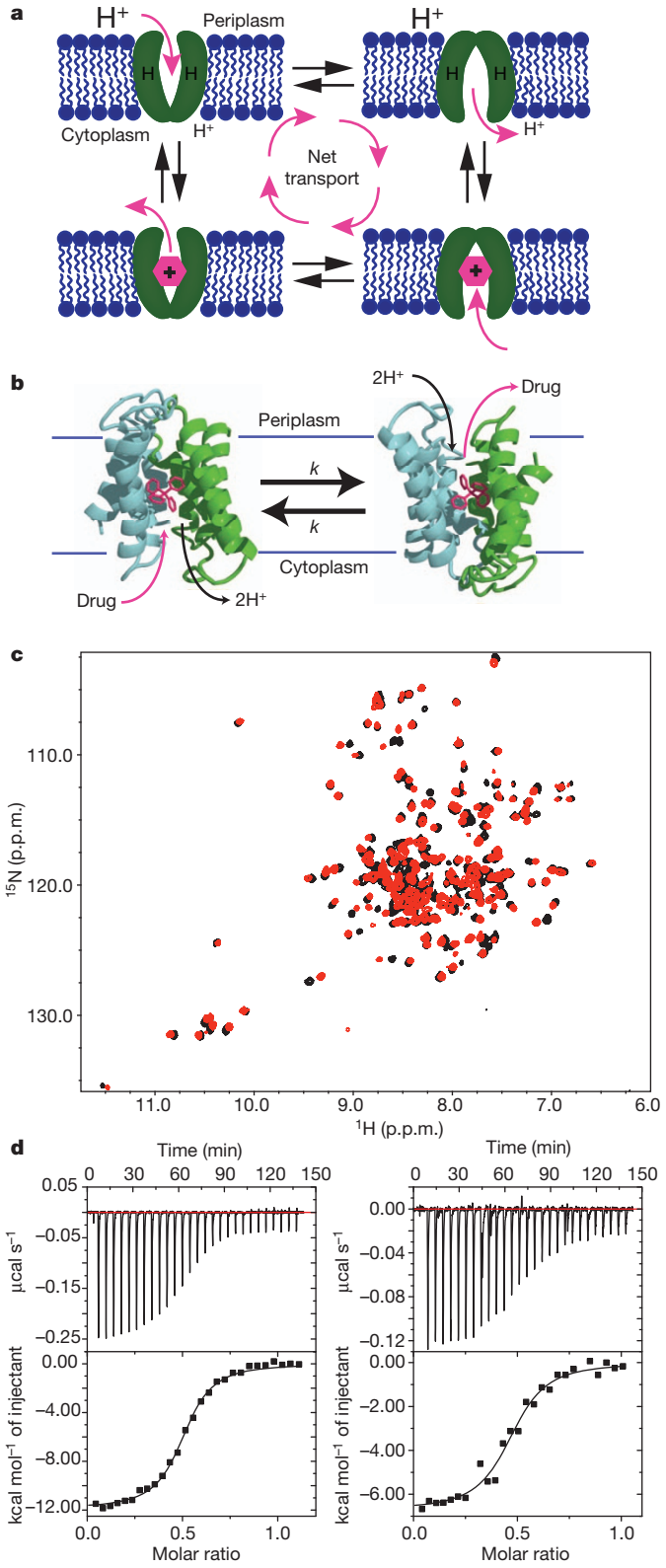

Figure 1 | Conformational interconversion and symmetry in the single-site alternating access model of EmrE transport. **a**, Each state in the transport cycle is only open to one side of the membrane, and the two states only interconvert when substrate (two protons or one polyaromatic cation) is bound. **b**, Conformational exchange as proposed for antiparallel, asymmetric EmrE[18]: the two monomers exchange conformations and the two states have identical structures. **c**, $^{1}H–^{15}N$ TROSY spectra of TPP^{+}-bound $^{2}H/^{15}N$-EmrE at pH 7, 45 °C, are nearly identical for DMPC/DHPC (black) or DLPC/DHPC (red) bicelles and are well resolved with twice as many peaks as expected for a monomer. **d**, EmrE is functional in isotropic bicelles. The affinity of EmrE for TPP^{+} is nearly identical in DMPC/DHPC isotropic bicelles (right) and DDM (left), as measured by ITC at pH 7, 45 °C.

dihexanoylphosphatidylcholine (DLPC/DHPC) or dimyristoylphosphatidylcholine/dihexanoylphosphatidylcholine (DMPC/DHPC) isotropic bicelles are nearly identical and characteristic of a folded protein. Spectra collected on TPP^{+}-bound EmrE solubilized in DDM micelles required longer acquisition time due to poor signal to noise, a pattern previously noted for other integral membrane proteins in DDM[32]. Nevertheless, the TROSY spectra (Supplementary Fig. 2) are remarkably similar in DDM and bicelles, and the key features of good chemical shift dispersion and peak doubling are preserved, confirming that the overall structure of EmrE is the same in both environments.

It is not possible to measure transport activity of solubilized protein, so substrate affinity is the best proxy for function. In a good environment EmrE is dimeric and binds TPP^{+} tightly[4,19,29,30,33] with the affinity weakening from dissociation constant $K_d \approx 2$ nM at pH 8.5 to 50 nM at pH 7 (DDM micelles, 4 °C)[19,20]. The pH-dependent TPP^{+} affinity is consistent with substrate competition between TPP^{+} and protons for the single binding site. In a poor environment, EmrE is monomeric and TPP^{+} binding weakens by three to four orders of magnitude[33,34]. Using isothermal titration calorimetry we confirmed that EmrE in DDM micelles at 4 °C binds TPP^{+} tightly, as previously reported[4,19,29,30,33] (Supplementary Fig. 3). At 45 °C, the temperature used for the NMR experiments, EmrE has the same affinity for TPP^{+} in DDM ($K_d = 120 \pm 12$ nM) or isotropic bicelles (170 ± 70 nM) at pH 7 (Fig. 1d and Supplementary Table 1). These values fall well within the variation observed for EmrE reconstituted into liposomes with different lipid composition[33]. The binding stoichiometry is 0.5 (one TPP^{+} per dimer), as expected, indicating that all the EmrE is functional in isotropic bicelles.

TPP^{+}-bound EmrE exchanges between two conformations

With the suitability of isotropic bicelles established, we turned to the key question: does TPP^{+}-bound EmrE interconvert between two states as predicted by the single-site alternating access model? To test this hypothesis we performed a TROSY-selected ZZ-exchange NMR experiment[35], modified to measure the dynamics of the protein without interference from the high lipid concentration in our samples (see Supplementary Information). In these experiments, the ^{15}N chemical shift of each amide is recorded, followed by a mixing period, and then the ^{1}H chemical shift is recorded. In the absence of conformational exchange, the spectrum observed will be identical to the TROSY spectrum. If conformational exchange between states A and B does occur during the mixing time, cross-peaks will appear in the ZZ-exchange spectrum at $^{15}N_A/^{1}H_B$ and $^{15}N_B/^{1}H_A$, forming a 'box' connecting the TROSY peaks corresponding to the chemical shifts of a single amide in state A ($^{15}N_A/^{1}H_A$) and state B ($^{15}N_B/^{1}H_B$) (Fig. 2a). It is immediately apparent that there is widespread conformational exchange with nearly every resolved TROSY peak assigned to exchange pairs. Analysing the peak volumes of the well-resolved exchange pairs reveals equal populations for both states (Supplementary Fig. 4), consistent with a concerted global exchange process.

The kinetics of conformational exchange can be directly determined by varying the mixing time and analysing cross-peak build-up and auto-peak decay as a function of time in the TROSY-selected ZZ-exchange experiment. Cross-peaks grow in and auto-peaks decay owing to exchange between states A and B, and all peaks decay because of the intrinsic relaxation (R^*) of the $S_Z I_\beta$ spin state active during the mixing time (see Supplementary Information)[35,36] according to

$$\frac{\mathrm{d}}{\mathrm{d}t}\begin{bmatrix} A \\ B \end{bmatrix} = \begin{bmatrix} -R^{*A} - k & k \\ k & -R^{*B} - k \end{bmatrix}\begin{bmatrix} A \\ B \end{bmatrix} \quad (1)$$

Because the populations are the same, the forward and reverse exchange rate constants are identical (k). Inspection of the data shows

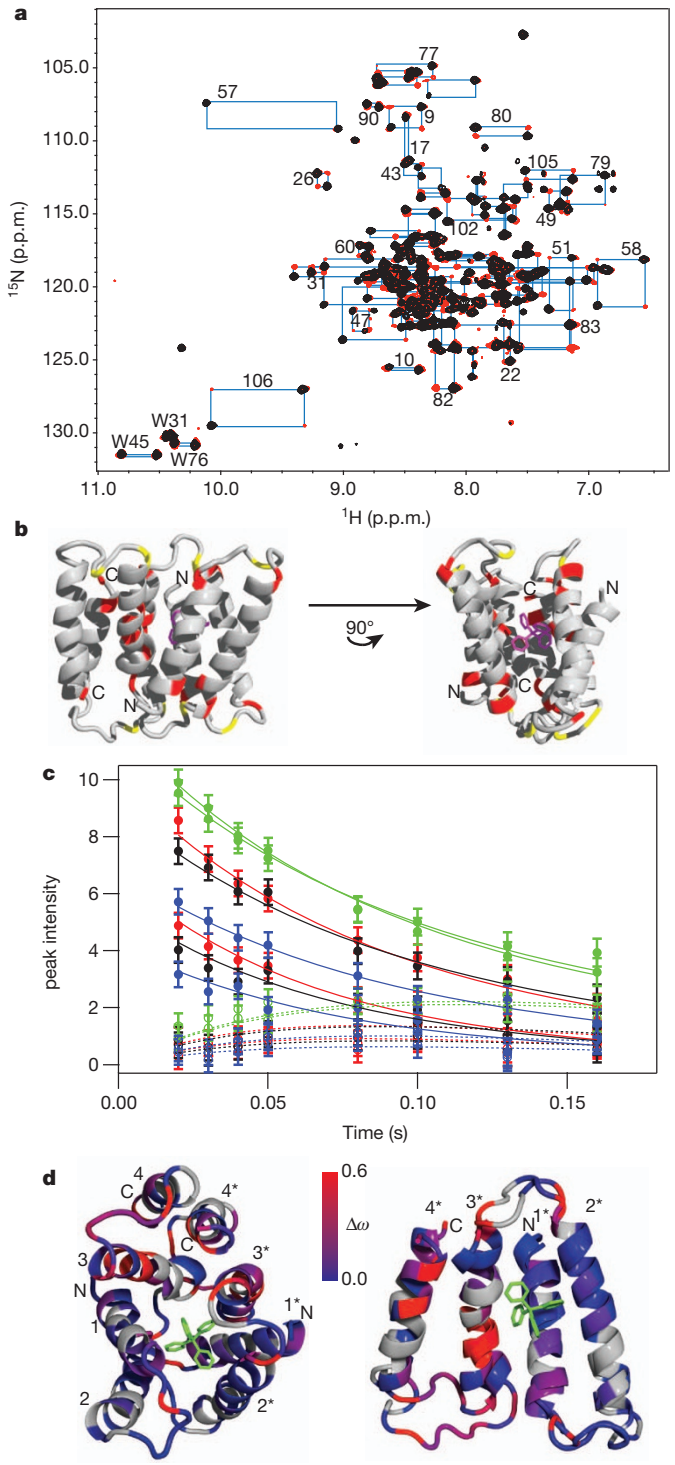

Figure 2 | TPP$^+$-bound EmrE interconverts between two conformations. **a**, Overlay of TROSY ZZ-exchange (red, 100 ms mixing time) and ^{1}H–^{15}N TROSY heteronuclear single-quantum coherence (HSQC) spectra (black) of TPP$^+$-bound ^{2}H/^{15}N-EmrE in isotropic bicelles. Cross-peaks demonstrate conformational exchange and blue boxes connect peaks corresponding to a single amide. All residues experience exchange. Assignments are shown for several well-resolved residues. **b**, Residues used for quantitative analysis are coloured based on whether the intrinsic relaxation rate is the same (red) or different (yellow) in the two states. **c**, Best fit of ZZ-exchange auto- (solid circles) and cross-peak (open circles) intensities as a function of mixing time (Supplementary equation (3)) yields a single global conformational exchange rate of $k = 4.9 \pm 0.5\ s^{-1}$. Each residue is a different colour (additional data in Supplementary Fig. 5). Error bars are estimated from the noise in each spectrum. **d**, Chemical shift difference ($\Delta\omega$) between states A and B (Supplementary equation (4)) are plotted onto the antiparallel dimer model (left) or an overlay of the two monomers with transmembrane helices 1–3 aligned to compare the two monomers within the antiparallel dimer (right).

quite clearly that the common assumption of equal intrinsic relaxation in both states ($R^{*A} = R^{*B}$) is not true for many residues (Fig. 2c and Supplementary Figs 5, 7 and 8). The Palmer group has developed an alternative method for analysing data that eliminates any effects of different R^* (ref. 37). The composite ratio of peak intensities (Ξ) calculated according to their method has a simple quadratic dependence on the mixing time (t), and in the case of equal populations $\Xi = k^2t^2$ (see Supplementary Information). For EmrE, analysis of Ξ shows that all residues collapse onto a single curve (Supplementary Fig. 6), confirming that this is a global conformational exchange process with a single timescale. Fitting the individual peak intensities as a function of time requires a more complex equation (Supplementary equation (3)), but results in the same global rate constant (Fig. 2c, Supplementary Fig. 5). This global conformational exchange rate is also detected in analysis of the tryptophan side chain dynamics (Supplementary Information and Supplementary Fig. 9).

These NMR dynamics experiments directly detect global conformational exchange between two states with equal populations and a rate constant of $k_{\text{open-in to open-out}} = k_{\text{open-out to open-in}} = k = 4.8 \pm 0.5\ s^{-1}$ for TPP$^+$-bound EmrE in isotropic bicelles at 45 °C. The atomic resolution provided by NMR demonstrates that the entire protein is involved in the conformational exchange process, as shown by the complete peak doubling. Importantly, the well-resolved residues used for quantitative analysis of the dynamics are distributed across the protein (Fig. 2b), indicating that the whole protein undergoes exchange on the same timescale. Second, residues with different intrinsic relaxation rates, R^*, map to the loop regions that alternate between a tightly packed protein environment and a loosely packed solvent-exposed environment as EmrE interconverts between inward- and outward-facing states, providing an explanation for the differential R^* (Supplementary Information). These results demonstrate the power of NMR methods to characterize quantitatively the kinetics (rate constants) and thermodynamics (populations) of global conformational exchange in a substrate-bound transporter, the key step for substrate transport across the membrane.

A previous study[20] monitoring intrinsic tryptophan fluorescence to measure substrate binding to EmrE detected an additional slow process with a rate constant of $1.5\ s^{-1}$ that was attributed to a conformational change after TPP$^+$ binding. Considering that the experiments were performed in different environments and at different temperatures, there is good agreement between the measured rates. This suggests both techniques are observing the same process and provides additional evidence that conformational exchange on this timescale in TPP$^+$-bound EmrE is an intrinsic property of the protein.

However, the topology of the exchanging EmrE is also needed to understand the molecular mechanism. Two possibilities are consistent with the NMR data (Supplementary Fig. 1): (1) parallel, symmetric EmrE dimers interconverting between inward- and outward-facing states (AA to BB exchange) and (2) the unique model of asymmetric antiparallel EmrE dimers interconverting between two states that are identical but open to opposite sides of the membrane (AB to BA exchange). With equal populations (1) requires two distinct EmrE conformations that happen to have exactly equal free energies, whereas (2) entails inherently equal populations because each dimer consists of one monomer in each conformation. To distinguish these two possibilities experimentally, we turned to Förster resonance energy transfer (FRET) experiments.

Antiparallel topology within EmrE dimers

There is still significant controversy about the topology of EmrE dimers. Several accessibility studies have shown that EmrE exists in both orientations in its native *E. coli* membrane[17,38]. Most recently,

Schuldiner and colleagues[17] have demonstrated equal populations of both monomer orientations in the native inner membrane of *E. coli* based on the accessibility of single cysteine residues to the outside of the cell. However, these studies do not directly address the relative orientation of monomers within the dimer. Structural studies consistently show an asymmetric antiparallel dimer[4,6,26,27,39,40]. Cross-linking of single-cysteine mutants and tandem genetic fusions have been used to enforce a parallel topology between monomers and these constructs are capable of transport[11,17]. However, an antiparallel genetic fusion is also capable of transport[17]. Charge bias mutants and fusion of fluorescent reporters provide more conflicting results, most probably because the topology is exquisitely sensitive to sequence alteration[16,17].

We performed bulk and single-molecule FRET and cross-linking experiments to determine the relative topology of EmrE monomers within a dimer. All the single-cysteine mutants used in these experiments are known to be functional[13,38,41]. In addition, two-dimensional $^{1}H–^{15}N$ TROSY spectra of TPP^{+}-bound mutants confirm that these single-cysteine mutants have the same structure as wild type (Supplementary Fig. 10). For bulk FRET measurements, we reconstituted single-cysteine EmrE mutants into liposomes to label specifically a single face of the protein (see Methods). To test for antiparallel topology, we labelled with donor and acceptor from opposite sides of the membrane (Fig. 3a). Significant acceptor fluorescence was observed upon donor excitation (Fig. 3c, red line), indicating FRET occurs and antiparallel dimers are present. To test for parallel topology, EmrE was labelled with both dyes from only one side of the membrane (Fig. 3b). Only minimal FRET was observed (Fig. 3c, blue line), which could be due to dye leakage into liposomes during labelling or a small population of higher-order oligomers (Supplementary Information and Supplementary Fig. 13). No FRET is observed in the control experiment (Fig. 3c, black line), demonstrating that monomers do not swap between dimers under these conditions.

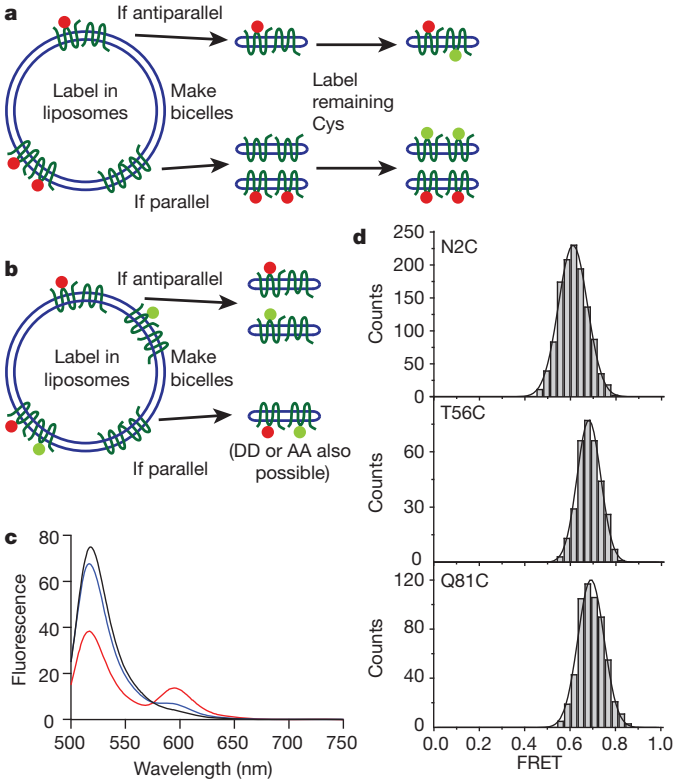

Figure 3 | EmrE is an antiparallel homodimer. T56C-EmrE was labelled in liposomes with two different schemes. **a**, Labelling with a single dye on each side of the membrane will produce FRET only if EmrE is antiparallel. **b**, Labelling with both donor and acceptor on the same side of the membrane will produce FRET only if EmrE is parallel. **c**, Observation of both donor (Alexa Fluor 488) and acceptor (Alexa Fluor 568) fluorescence upon donor excitation in sample **a** indicates FRET and antiparallel topology (red line). In contrast, only minimal FRET was observed in sample **b** (blue line). The control (black line, see Methods) excludes monomer swapping and direct excitation of acceptor. All fluorescence spectra are normalized to total donor fluorescence in SDS, which monomerizes EmrE[49]. **d**, For single-molecule FRET experiments, N2C-, T56C- or Q81C-EmrE was labelled with Cy3/Cy5 in micelles and then reconstituted into bicelles. Particles containing one donor and one acceptor were selected based on photobleaching events. A single, narrow FRET distribution is observed in each case, with a FRET efficiency consistent with an antiparallel topology.

To simplify labelling and avoid leakage issues, we used single-molecule FRET[42]. Single-cysteine EmrE was stoichiometrically labelled with Cy3/Cy5 in micelles at one of three different positions, N2C, T56C or Q81C (Supplementary Fig. 11), followed by incorporation into bicelles. These bicelles contained 0.1% biotinylated lipid to tether specifically Cy3/Cy5-EmrE-containing bicelles to neutravidine molecules on the polymer-coated slide surface (Supplementary Fig. 11). The single-molecule FRET experiments were performed with a wide-field total internal reflection fluorescence microscope set up[43]. Observation of photobleaching events during single molecule time traces allows dimers to be selected that contain one donor and one acceptor fluorophore. A single FRET distribution is observed for single-site labelled EmrE (Fig. 3d). The FRET efficiency of 0.6–0.7, depending on labelling site, corresponds to a distance of approximately 50–55 Å, consistent with transmembrane labelling. Based on the dimensions of the cryo-electron microscopy structure, donor and acceptor would not be more than about 35 Å apart, corresponding to a FRET efficiency greater than 0.9, if they were on the same side of the membrane as required for a parallel topology with this labelling scheme. These results confirm the antiparallel arrangement of monomers within an EmrE dimer.

To test this model further, we cross-linked S107C-EmrE with the heterobifunctional cross-linker sulpho-(*N*-(γ-maleimidobutyryloxy) succinimide) (s-GMBS). Nearly complete cross-linking is observed (Supplementary Fig. 14), demonstrating that residues K22 and S107C are in close proximity in the dimer. Because these positions are on opposite sides of the membrane in each monomer, heterobifunctional cross-linking is only possible with an antiparallel topology (Supplementary Information and Supplementary Fig. 14). Together with the NMR results, this means that TPP^{+}-bound EmrE must exist in an antiparallel asymmetric dimer that interconverts between two identical, oppositely oriented states (AB–BA dimer exchange) when bound to TPP^{+} (Supplementary Fig. 1).

According to this model, no conformational exchange should be observed in the single molecule FRET time traces, because the donor–acceptor distance will be identical in both states. Inspection of the time traces confirms this prediction (Supplementary Fig. 12), even though the rate of conformational exchange determined by NMR is within the range observable in these experiments. Our NMR spectra are very clean, with the double set of peaks fully accounted for by a single population of antiparallel EmrE. We do not observe additional minor peaks (Supplementary Fig. 1), so parallel EmrE is not present in our samples in measurable amounts (less than 5%).

The single-site alternating access model predicts that the two lowest energy states in the TPP^{+}-bound conformation are the inward- and outward-facing states. If EmrE is open to one side of the membrane in our NMR samples, then we should observe different water accessibility for residues at the loops and ends of helices upon exchange from state A to state B because these regions pack together to close off the active site of EmrE at one end and open up to allow access to the active site at the other. To test this, we recorded $^{1}H–^{15}N$ TROSY spectra with increasing concentrations of a soluble, chelated gadolinium compound. This paramagnetic compound causes line broadening of nearby amides. The results (Fig. 4a) show that some amides are similarly affected in both states whereas others are differentially broadened. The amides with differential accessibility to water map exactly to the regions expected for interconversion of an antiparallel dimer between 'symmetric' states (Fig. 1b and Supplementary Fig. 1), confirming that the conformation

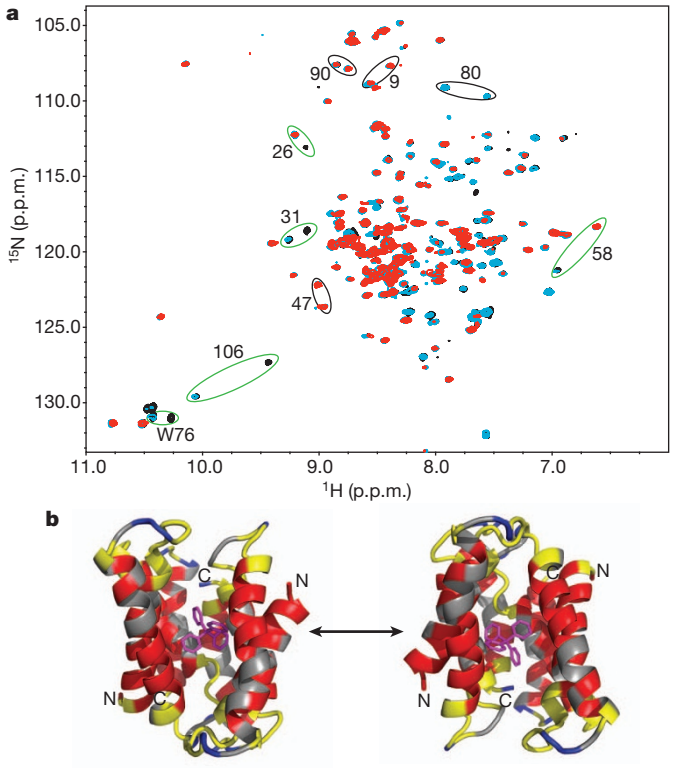

Figure 4 | EmrE has asymmetric water accessibility. **a**, ^{1}H–^{15}N TROSY spectra of TPP^{+}-bound EmrE in bicelles in the absence (black) and presence of 1 mM (blue) and 5 mM (red) paramagnetic gadobenate dimeglumine. Residues with different PRE effects (green circles) or the same PRE effect (black circles) in the two states are highlighted. **b**, Residues with equal accessibility (dark blue) or protection (red) from water in both states are plotted on the structure. Grey residues are not assigned in both states. Residues with differential accessibility to water (yellow) highlight the pore and loop regions, exactly as expected for inward- to outward-facing conformational exchange. This is consistent with an antiparallel dimer open only to one side of the membrane, as in the crystal structure (Protein Data Bank accession number 3B5D).

we observe is open to one side of the membrane and is consistent with the crystal structure (Fig. 4b).

The ZZ-exchange data assign pairs of peaks as exchange partners, representing the chemical shift of a single residue in each state. Chemical shift is quite sensitive to local structural changes. In the conformational exchange model proposed for EmrE, the two monomers swap conformations during the transition from inward- to outward-facing states (AB–BA). Thus, overlay of the two monomers (Fig. 2d) highlights regions where local structure changes upon conformational exchange in this model. The overlay reveals kinking of transmembrane helix 3 and movement of transmembrane helix 4 relative to the substrate-binding domain as the largest structural changes. This is exactly where the largest chemical shift differences between the two states (Supplementary equation (4)) are observed. The transmembrane helices lining the binding pocket move as a generally rigid body, with significant chemical shift differences only in the regions that close off or open up access to the transport pore (Fig. 2d). These chemical shift differences are entirely consistent with the structural differences between the two monomers, supporting the AB–BA exchange model. The two sets of NMR peaks correspond to the two distinct monomer conformations within an exchanging antiparallel asymmetric dimer.

Antiparallel EmrE is competent for transport

We have used solution NMR spectroscopy to observe directly conformational exchange between inward- and outward-facing states of the small multidrug resistance transporter, EmrE. This is the key step in the transport cycle that moves the substrate across the membrane from one aqueous compartment to another. Measurement of bulk transport is not possible in a solubilized system. However, solution NMR provides a powerful tool to follow directly the protein conformational changes that effectively 'transport' TPP^{+}, and we have quantitatively measured this exchange process in TPP^{+}-bound EmrE.

Our FRET experiments show that the monomers within each dimer are antiparallel. Thus, antiparallel substrate-bound EmrE is able to undergo the key conformational exchange step in the single-site alternating access model of antiport. Together with our chemical shift mapping and water accessibility data, this suggests that the low-resolution crystal and cryo-electron microscopy structures are essentially correct, and we are working to refine and improve the resolution of this structure using NMR restraints.

Our results provide experimental evidence for the unusual model proposed by Fleishman *et al.* that the inward- and outward-facing states are identical[18] (Supplementary Fig. 1). This model reconciles the asymmetric antiparallel structural data[4,6,26,27,39,40] with biochemical studies indicating functional symmetry of active site residues[3,44,45] and single distances measured for most residues by electron paramagnetic resonance (EPR)[13]. These results demonstrate that equal insertion of EmrE in both orientations in the *E. coli* inner membrane[17] is functionally relevant and they enhance the importance of EmrE as a potential model for evolution of dual topology membrane proteins[9].

METHODS SUMMARY

EmrE was expressed and purified using a 6× His-tag, which was then removed with thrombin. Purification was performed in decylmaltoside or DDM. EmrE was reconstituted into DMPC or DLPC liposomes using standard methods and then formed into isotropic bicelles by addition of DHPC and several freeze–thaw cycles. Protein concentration was determined using absorbance at 280 nm, with an extinction coefficient determined by amino-acid analysis. Isothermal titration calorimetry (ITC) was performed by titrating 54 μM TPP^{+} stock solutions into 10 μM EmrE, with matching concentrations of detergent or lipid in both solutions.

Bulk FRET labelling was performed in liposomes to label residues separately on either side of the membrane. An 'antiparallel' sample was labelled with donor and acceptor on opposite sides, and a 'parallel' sample was labelled with donor and acceptor on the same side. Donor-only and acceptor-only controls were labelled with dye only on the exterior of the liposome, reconstituted into bicelles and then mixed. Single-molecule FRET samples were labelled in micelles and experiments were performed using a wide-field total internal reflection fluorescence microscope set up[43].

NMR experiments were performed using a 700 MHz Varian NMR spectrometer or 800 MHz Bruker spectrometer equipped with a cryoprobe. All NMR samples contained 0.5–1.0 mM ^{2}H/^{15}N-EmrE in buffer conditions of 2 mM TPP^{+}, 20 mM NaCl, 20 mM potassium phosphate, 2 mM TCEP, pH 7.0, 45 °C. The membrane mimetic in each sample (DDM micelles or isotropic bicelles) was as listed. The TROSY-selected ZZ-exchange experiment[35] was modified to include a lipid 'flipback' pulse. Data were processed and analysed with NMRPipe[46], NMRView[47], Sparky[48] and IgorPro (Wavemetrics). All EmrE structure figures were created in PyMOL using Protein Data Bank 3B5D with the backbone rebuilt to render the cartoons. Full-page versions of the spectra in the main figures are included in the Supplementary Information.

Full Methods and any associated references are available in the online version of the paper at www.nature.com/nature.

Received 20 January; accepted 7 November 2011.
Published online 18 December 2011.

1. Arkin, I. T., Russ, W. P., Lebendiker, M. & Schuldiner, S. Determining the secondary structure and orientation of EmrE, a multi-drug transporter, indicates a transmembrane four-helix bundle. *Biochemistry* **35,** 7233–7238 (1996).
2. Yerushalmi, H., Lebendiker, M. & Schuldiner, S. EmrE, an *Escherichia coli* 12-kDa multidrug transporter, exchanges toxic cations and H^{+} and is soluble in organic solvents. *J. Biol. Chem.* **270,** 6856–6863 (1995).
3. Schuldiner, S. EmrE, a model for studying evolution and mechanism of ion-coupled transporters. *Biochim. Biophys. Acta* **1794,** 748–762 (2009).
4. Tate, C. G., Ubarretxena-Belandia, I. & Baldwin, J. M. Conformational changes in the multidrug transporter EmrE associated with substrate binding. *J. Mol. Biol.* **332,** 229–242 (2003).
5. Butler, P. J., Ubarretxena-Belandia, I., Warne, T. & Tate, C. G. The *Escherichia coli* multidrug transporter EmrE is a dimer in the detergent-solubilised state. *J. Mol. Biol.* **340,** 797–808 (2004).

6. Ubarretxena-Belandia, I. & Tate, C. G. New insights into the structure and oligomeric state of the bacterial multidrug transporter EmrE: an unusual asymmetric homo-dimer. *FEBS Lett.* **564,** 234–238 (2004).
7. Chen, Y. J. *et al.* X-ray structure of EmrE supports dual topology model. *Proc. Natl Acad. Sci. USA* **104,** 18999–19004 (2007).
8. Ninio, S., Elbaz, Y. & Schuldiner, S. The membrane topology of EmrE – a small multidrug transporter from *Escherichia coli*. *FEBS Lett.* **562,** 193–196 (2004).
9. Rapp, M., Seppälä, S., Granseth, E. & von Heijne, G. Emulating membrane protein evolution by rational design. *Science* **315,** 1282–1284 (2007).
10. McHaourab, H. S., Mishra, S., Koteiche, H. A. & Amadi, S. H. Role of sequence bias in the topology of the multidrug transporter EmrE. *Biochemistry* **47,** 7980–7982 (2008).
11. Steiner-Mordoch, S. *et al.* Parallel topology of genetically fused EmrE homodimers. *EMBO J.* **27,** 17–26 (2008).
12. Korkhov, V. M. & Tate, C. G. An emerging consensus for the structure of EmrE. *Acta Crystallogr. D* **65,** 186–192 (2009).
13. Amadi, S. T., Koteiche, H. A., Mishra, S. & McHaourab, H. S. Structure, dynamics and substrate-induced conformational changes of the multidrug transporter EmrE in liposomes. *J. Biol. Chem.* **285,** 26710–26718 (2010).
14. Soskine, M., Mark, S., Tayer, N., Mizrachi, R. & Schuldiner, S. On parallel and antiparallel topology of a homodimeric multidrug transporter. *J. Biol. Chem.* **281,** 36205–36212 (2006).
15. Charalambous, K., Miller, D., Curnow, P. & Booth, P. J. Lipid bilayer composition influences small multidrug transporters. *BMC Biochem.* **9,** 31 (2008).
16. Seppala, S., Slusky, J., Lloris-Garcera, P., Rapp, M. & Von Heijne, G. Control of membrane protein topology by a single C-terminal residue. *Science* **328,** 1698–1700 (2010).
17. Nasie, I., Steiner-Mordoch, S., Gold, A. & Schuldiner, S. Topologically random insertion of EmrE supports a pathway for evolution of inverted repeats in ion-coupled transporters. *J. Biol. Chem.* **285,** 15234–15244 (2010).
18. Fleishman, S. J. *et al.* Quasi-symmetry in the cryo-EM structure of EmrE provides the key to modeling its transmembrane domain. *J. Mol. Biol.* **364,** 54–67 (2006).
19. Yerushalmi, H. & Schuldiner, S. A model for coupling of H^+ and substrate fluxes based on 'time-sharing' of a common binding site. *Biochemistry* **39,** 14711–14719 (2000).
20. Adam, Y., Tayer, N., Rotem, D., Schreiber, G. & Schuldiner, S. The fast release of sticky protons: kinetics of substrate binding and proton release in a multidrug transporter. *Proc. Natl Acad. Sci. USA* **104,** 17989–17994 (2007).
21. Jardetzky, O. Simple allosteric model for membrane pumps. *Nature* **211,** 969–970 (1966).
22. West, I. C. Ligand conduction and the gated-pore mechanism of transmembrane transport. *Biochim. Biophys. Acta* **1331,** 213–234 (1997).
23. Glover, K. J. *et al.* Structural evaluation of phospholipid bicelles for solution-state studies of membrane-associated biomolecules. *Biophys. J.* **81,** 2163–2171 (2001).
24. Whiles, J., Ceems, R. & Vold, R. Bicelles in structure–function studies of membrane-associated proteins. *Bioorg. Chem.* **30,** 431–442 (2002).
25. Raschle, T., Hiller, S., Etzkorn, M. & Wagner, G. Nonmicellar systems for solution NMR spectroscopy of membrane proteins. *Curr. Opin. Struct. Biol.* **20,** 471–479 (2010).
26. Lehner, I. *et al.* The key residue for substrate transport (Glu14) in the EmrE dimer is asymmetric. *J. Biol. Chem.* **283,** 3281–3288 (2008).
27. Ubarretxena-Belandia, I., Baldwin, J. M., Schuldiner, S. & Tate, C. G. Three-dimensional structure of the bacterial multidrug transporter EmrE shows it is an asymmetric homodimer. *EMBO J.* **22,** 6175–6181 (2003).
28. Rotem, D. & Schuldiner, S. EmrE, a multidrug transporter from *Escherichia coli*, transports monovalent and divalent substrates with the same stoichiometry. *J. Biol. Chem.* **279,** 48787–48793 (2004).
29. Soskine, M., Adam, Y. & Schuldiner, S. Direct evidence for substrate-induced proton release in detergent-solubilized EmrE, a multidrug transporter. *J. Biol. Chem.* **279,** 9951–9955 (2004).
30. Yerushalmi, H., Mordoch, S. S. & Schuldiner, S. A single carboxyl mutant of the multidrug transporter EmrE is fully functional. *J. Biol. Chem.* **276,** 12744–12748 (2001).
31. Muth, T. R. & Schuldiner, S. A membrane-embedded glutamate is required for ligand binding to the multidrug transporter EmrE. *EMBO J.* **19,** 234–240 (2000).
32. Sanders, C. R. & Sönnichsen, F. Solution NMR of membrane proteins: practice and challenges. *Magn. Reson. Chem* **44** (*NMR of Proteins in Solution* special issue) S24–S40 (2006).
33. Miller, D. *et al. In vitro* unfolding and refolding of the small multidrug transporter EmrE. *J. Mol. Biol.* **393,** 815–832 (2009).
34. Sikora, C. W. & Turner, R. J. Investigation of ligand binding to the multidrug resistance protein EmrE by isothermal titration calorimetry. *Biophys. J.* **88,** 475–482 (2005).
35. Li, Y. & Palmer, A. G. TROSY-selected ZZ-exchange experiment for characterizing slow chemical exchange in large proteins. *J. Biomol. Nucl. Magn. Reson.* **45,** 357–360 (2009).
36. Farrow, N. A., Zhang, O., Forman-Kay, J. D. & Kay, L. E. A heteronuclear correlation experiment for simultaneous determination of ^{15}N longitudinal decay and chemical exchange rates of systems in slow equilibrium. *J. Biomol. Nucl. Magn. Reson.* **4,** 727–734 (1994).
37. Miloushev, V. Z. *et al.* Dynamic properties of a type II cadherin adhesive domain: implications for the mechanism of strand-swapping of classical cadherins. *Structure* **16,** 1195–1205 (2008).
38. Nara, T. *et al.* Anti-parallel membrane topology of a homo-dimeric multidrug transporter, EmrE. *J. Biochem.* **142,** 621–625 (2007).
39. Korkhov, V. M. & Tate, C. G. Electron crystallography reveals plasticity within the drug binding site of the small multidrug transporter EmrE. *J. Mol. Biol.* **377,** 1094–1103 (2008).
40. Agarwal, V., Fink, U., Schuldiner, S. & Reif, B. MAS solid-state NMR studies on the multidrug transporter EmrE. *Biochim. Biophys. Acta* **1768,** 3036–3043 (2007).
41. Mordoch, S. S., Granot, D., Lebendiker, M. & Schuldiner, S. Scanning cysteine accessibility of EmrE, an H+-coupled multidrug transporter from *Escherichia coli*, reveals a hydrophobic pathway for solutes. *J. Biol. Chem.* **274,** 19480–19486 (1999).
42. Ha, T. *et al.* Probing the interaction between two single molecules: fluorescence resonance energy transfer between a single donor and a single acceptor. *Proc. Natl Acad. Sci. USA* **93,** 6264–6268 (1996).
43. Roy, R., Hohng, S. & Ha, T. A practical guide to single-molecule FRET. *Nature Methods* **5,** 507–516 (2008).
44. Sharoni, M., Steiner-Mordoch, S. & Schuldiner, S. Exploring the binding domain of EmrE, the smallest multidrug transporter. *J. Biol. Chem.* **280,** 32849–32855 (2005).
45. Weinglass, A. B. *et al.* Exploring the role of a unique carboxyl residue in EmrE by mass spectrometry. *J. Biol. Chem.* **280,** 7487–7492 (2005).
46. Delaglio, F. *et al.* NMRPipe: a multidimensional spectral processing system based on UNIX pipes. *J. Biomol. Nucl. Magn. Reson.* **6,** 277–293 (1995).
47. Johnson, B. A. & Blevins, R. A. NMRView: a computer program for the visualization and analysis of NMR data. *J. Biomol. Nucl. Magn. Reson.* **4,** 603–614 (1994).
48. Goddard, T. D. & Kneller, D. G. Sparky 3. University of California, San Francisco.
49. Rotem, D., Sal-man, N. & Schuldiner, S. *In vitro* monomer swapping in EmrE, a multidrug transporter from *Escherichia coli*, reveals that the oligomer is the functional unit. *J. Biol. Chem.* **276,** 48243–48249 (2001).

Supplementary Information is linked to the online version of the paper at www.nature.com/nature.

Acknowledgements We thank Y. Liu for assistance replicating the ITC data. We thank J. Villali for assistance growing isotopically labelled EmrE. We are grateful to Y. Li and A. Palmer for providing pulse programs and G. Chang for providing the EmrE expression plasmid. This work was supported by the National Institutes of Health (1R01GM095839) and the Searle Scholars Program (K.H.W.), the US Department of Energy, Office of Basic Energy Sciences (D.K.), the Howard Hughes Medical Institute (D.K. and T.H.), and an NSF graduate research fellowship to E.M. (DGE-1143954).

Author Contributions E.M. and K.H.W. optimized EmrE sample preparation, performed ITC experiments and recorded two-dimensional NMR spectra under different conditions. E.M. and G.D. performed the bulk FRET experiments. S.D. and R.V. performed the single molecule FRET experiments with guidance from T.H. G.D. and M.C. optimized the modified ZZ-exchange NMR experiment. M.C. collected the ZZ-exchange data and K.H.W. analysed it. G.D. performed the paramagnetic relaxation enhancement NMR experiments. A.B., E.M., G.D. and K.H.W. contributed to assignments. D.K. mentored initial project development. K.H.W. conceived the project and wrote the manuscript.

Author Information Reprints and permissions information is available at www.nature.com/reprints. The authors declare no competing financial interests. Readers are welcome to comment on the online version of this article at www.nature.com/nature. Correspondence and requests for materials should be addressed to K.H.W. (khenzler@wustl.edu).

METHODS

EmrE expression and purification. EmrE was expressed using a pET15b plasmid provided by G. Chang[7]. This vector produces EmrE with an amino (N)-terminal 6× His tag that can be removed by cleavage with thrombin to leave only two extra N-terminal residues (GS). BL21(DE3) cells transformed with this vector were grown in M9 minimal media. EmrE was induced with 0.33 mM IPTG at an absorbance $A_{600\,nm}$ of 0.7–0.8 at 17 °C. Cells were collected after 14–20 h. $^{1}H/^{15}N$-labelled EmrE was produced in the same way substituting 1 g $^{15}NH_4Cl$. $^{2}H/^{15}N$-labelled EmrE was produced by growing cells in $^{2}H/^{15}N$ M9 (1 g $^{15}NH_4Cl$, 2 g glucose, 12.8 g $Na_2HPO_4{\cdot}7H_2O$, 3.0 g KH_2PO_4, 0.5 g NaCl, 2 ml 1 M $MgSO_4$ in D_2O, 100 µl 1 M $CaCl_2$in D_2O, 100 mg ampicillin, one generic multivitamin, 0.5 g $^{2}H/^{15}N$ Isogro (Sigma) per litre).

Cell pellets were re-suspended in lysis buffer (100 mM NaCl, 2.5 mM $MgSO_4$, 20 mM tris pH 7.5, 250 mM sucrose, 5 mM β-mercaptoethanol, 1 mg ml^{-1} lysozyme, DNase, 1 µg ml^{-1} pepstatin, 10 µM leupeptin and 100 µM PMSF) and lysed by sonication. The membrane fraction was separated by a high-speed spin (30,000*g* for 1 h), re-suspended in the same buffer and solubilized with 40 mM decylmaltoside (Anatrace) at room temperature for 2 h. After a second high-speed spin, the supernatant was applied to Ni-NTA His•Bind beads (Novagen) prewashed with buffer A (10 mM decylmaltoside, 10 mM KCl, 90 mM NaCl, 20 mM tris, pH 7.8, 5 mM β-mercaptoethanol) and allowed to bind for 15 min at room temperature. The beads were washed with 10 bed volumes of buffer A, followed by 10 bed volumes of buffer B (buffer A plus 5 mM imidazole). EmrE was eluted with five bed volumes of elution buffer (buffer A plus 400 mM imidazole). The salt concentration was increased to 200 mM and thrombin was added to cleave the His-tag overnight at room temperature. Samples were then concentrated and 0.5 ml aliquots loaded onto a Superdex 200 column pre-equilibrated in NMR buffer (20 mM potassium phosphate, 20 mM NaCl, pH 7.0) with 10 mM decylmaltoside. The protein eluted near 14–15 ml with a symmetric peak. Fractions containing EmrE were combined and reconstituted into bicelles. For samples in DDM (Anatrace), DDM was substituted for decylmaltoside throughout the protocol and the fast protein liquid chromatography fractions were combined and concentrated to the desired final protein/detergent concentration.

Preparation of isotropic bicelles. First, the amount of EmrE in the combined fast protein liquid chromatography fractions was determined as described below. Long-chain lipid (DLPC (1,2-dilauroyl-*sn*-glycero-3-phosphocholine) or DMPC (1,2-dimyristoyl-*sn*-glycero-3-phosphocholine), Avanti Polar Lipids) was hydrated in NMR buffer at 20 mg ml^{-1}. At least 200:1 molar ratio of lipid:EmrE dimer was used for all samples. The lipids were bath sonicated for 10 min and 50 µl of 10% octyl glucoside (Anatrace) was added per millitre of solution. After 20 min, they were mixed with the fast protein liquid chromatography fractions containing EmrE and incubated for 30 min. Three aliquots of 30 mg BioBeads (BioRad) per milligram of total detergent were used to remove the detergent. After removal of the BioBeads, the vesicles were collected by ultracentrifugation at 50,000*g* for 1 h at 20 °C. The supernatant was removed and the pellet was re-suspended in NMR buffer containing DHPC (1,2-dihexanoyl-*sn*-glycero-3-phosphocholine, Avanti Polar Lipids) to break the liposomes up into bicelles. The DHPC concentration was calculated to produce a 1:3 ratio of long-chain lipid:DHPC, assuming 85% recovery of long-chain lipid. Four freeze–thaw cycles were used to produce uniform bicelles; samples were stored at −80 °C until use.

EmrE concentration determination. EmrE concentration was determined using absorbance at 280 nm. The extinction coefficient (38,370 l mol^{-1} cm^{-1}) was calibrated using amino-acid analysis of three samples of EmrE each in DDM and decylmaltoside, and was found to be the same for EmrE in bicelles.

ITC. ITC experiments were performed using a VP-ITC titration microcalorimeter (MicroCal) by titrating TPP^+ (50–80 µM) into EmrE (9–13 µM) in isotropic bicelles ($q = 0.33$, DMPC/DHPC) or 5 mM analytical grade DDM. Both the TPP^+ and EmrE solution were in NMR buffer and had matching detergent or lipid concentrations. Matching bicelle stocks were produced by acquiring proton NMR spectra of all samples (empty bicelle blank, TPP^+ stock, EmrE stock), integrating the DMPC and DHPC terminal methyl peaks, and ensuring that the lipid ratio and peak volumes matched. Isotropic bicelle samples had a total lipid concentration of 30–50 mM and $q_{effective} = 0.33$[23]. The TPP^+ concentration in the final stock solution was determined spectrophotometrically ($\varepsilon = 4{,}400$ l mol^{-1} cm^{-1} at 269 nm, 3,750 l mol^{-1} cm^{-1} at 276 nm). Heats of dilution were determined from reference titrations of the same TPP^+ stock into empty micelles or bicelles. Data were fitted to a model of the ligand TPP^+ (X) binding to n independent and identical sites on the macromolecule EmrE (M) to determine the association constant (K), enthalpy of binding (ΔH) and binding stoichiometry (n), using equation (1):

$$Q_i^{tot} = V_o \Delta H \bullet M_i^{tot} \frac{nKx}{1+Kx} \qquad (2)$$

where x is the free ligand concentration, M_i^{tot} is the total macromolecule concentration, Q_i^{tot} is total heat after the ith injection and V_o is the cell volume. The data were fitted with a nonlinear least-squares approach using the ITC Data Analysis in Origin software supplied with the calorimeter (OriginLab).

Error was determined from standard deviation between replicate experiments. The K values from each replicate were averaged, and then the average value was converted to the dissociation constant, K_d.

Bulk FRET sample preparation and measurement. All FRET and cross-linking experiments use single-cysteine mutants of EmrE: the three native cysteines are mutated to serine and a single cysteine is introduced at the desired location. T56C-EmrE was reduced with DTT and then reconstituted into DMPC liposomes with a molar ratio at least 300:1 lipid:EmrE monomer. After ultracentrifugation to collect the liposomes, they were re-suspended in deoxygenated NMR buffer with 2 mM cysteine and extruded through 400 µm filters to produce unilamellar vesicles loaded with cysteine. The sample was passed over a G25 Sephadex column to remove free cysteine from the exterior of the liposomes. The tight-binding substrate TPP^+ was maintained at saturating concentrations throughout the preparation to stabilize EmrE dimers and prevent monomer swapping.

To test for antiparallel topology, the first dye-maleimide was added to the exterior of the liposomes at 5× molar ratio relative to EmrE monomer. The reaction was allowed to proceed for 30 min, then quenched by addition of 20-fold excess of β-mercaptoethanol. Free dye was removed by collecting the liposomes by ultracentrifugation, re-suspending in fresh buffer and repeating the ultracentrifugation. The second dye-maleimide was added along with octyl glucoside to disrupt the liposomes. The reaction was allowed to proceed for 1 h and then quenched as before. Free dye and detergent were removed by passing the sample over a second G25 Sephadex column. DHPC was then added to the liposome suspension to form bicelles. Alexa Fluor 488 was used as the donor and Alexa Fluor 568 as the acceptor for bulk FRET experiments.

To test for parallel topology, samples were produced in a similar manner, but labelled with mixed donor and acceptor only from the exterior of the liposome. After the labelling reaction, remaining free dye was quenched and removed, then DHPC added to form bicelles. This should produce EmrE with only one face labelled by fluorescent dye, and any cysteine that faces the interior of the liposome should remain unlabelled. Two additional control samples were independently labelled with either donor only or acceptor only from the exterior of the liposome and then mixed.

Fluoresence measurements were made using a PTI spectrofluorimeter (Photon Technology International) using FeliX fluorescence analysis software version 1.42b (Photon Technology International). Labelled T56C-EmrE samples were diluted into isotropic bicelles or 5% SDS containing 2 mM TPP^+. The donor, Alexa Fluor 488 was excited at a wavelength of 488 nm and emission spectra were collected scanning from 500 to 750 nm. The acceptor, Alexa Fluor 568, was excited at a wavelength of 568 nm and emission spectra were collected scanning from 580 to 750 nm.

Single-molecule FRET experiments. Three different single-cysteine mutants, N2C, Q81C and T56C, were labelled with Cy3-maleimide and Cy5-maleimide for single-molecule FRET experiments. Labelling was performed in the same manner as bulk FRET samples, or by labelling EmrE in detergent micelles using an equimolar mixture of donor and acceptor before reconstitution into isotropic bicelles as previously described. The final bicelles used for single-molecule FRET experiments contained 0.1% biotinyl-DPPE for immobilizing the samples.

Single-molecule experiments were performed on a wide-field total internal reflection fluorescence microscope set up[43]. Biotinylated bicelles containing Cy3 and Cy5 labelled EmrE were specifically immobilized on a polymer-coated quartz surface. Then free bicelles were flushed out of the chamber and molecules were imaged in the imaging buffer consisting of 3 mM Trolox and the oxygen scavenger system (0.8% dextrose, 0.1 mg ml^{-1} glucose oxidase, 0.02 mg ml^{-1} catalase) in NMR buffer (2 mM TPP^+, 20 mM NaCl, 20 mM potassium phosphate, pH 7.0). A 532 green laser (Coherent) was used for Cy3 excitation and the sample was imaged by a charge-coupled-device camera (iXon DV 887-BI; Andor Technology). Homemade IDL and C++ programs were used to record and analyse the movies. FRET efficiency was calculated from $I_A/(I_D + I_A)$, where I_D and I_A are the donor (Cy3) and acceptor (Cy5) fluorescent intensities respectively.

For each sample, several minute-long movies were collected (imaging area 70 µm× 35 µm) at 100 ms time resolution. Donor and acceptor intensity time traces were corrected for the background and smoothed using four-point adjacent-averaging. FRET efficiencies from molecules that showed single Cy3 and Cy5 photobleaching steps were chosen to build the histograms.

Cross-linking of EmrE. *o*-PDM (*N*,*N*′-(*o*-phenylene)dimaleimide) and s-GMBS were used to cross-link S107C EmrE to test for parallel (*o*-PDM) or antiparallel (s-GMBS) topology. These experiments were performed with 90 µM EmrE,

20 mM potassium phosphate, 20 mM sodium chloride, 1 mM TCEP, pH 7, and cross-linking for 20 min at 37 °C followed by quenching with β-mercaptoethanol at 20× the cross-linker concentration. Cross-linking in detergent was performed in 10 mM decylmaltoside; cross-linking in lipid was performed in DLPC liposomes at the specified protein:lipid ratio. Addition of SDS monomerizes EmrE and provides a control. S107/K22R serves as a control to determine whether the lysine side chain or N-terminal amine participates in the s-GMBS cross-linking reaction.

NMR sample preparation and data acquisition. All NMR samples were 0.5–1.0 mM $^{2}H/^{15}N$-EmrE, and contained excess (2 mM) TPP^{+} to saturate the protein with substrate. The sample in DDM (Supplementary Fig. 1) had 118 mM DDM. All other NMR samples were isotropic bicelles as described above, with at least 100:1 long-chain lipid:EmrE molar ratio, total lipid concentrations of 300–400 mM and $q \approx 0.33$. The q value was confirmed for each sample by integrating the DMPC (or DLPC) and DHPC methyl resonances. All NMR samples were prepared in 20 mM potassium phosphate, 20 mM NaCl buffer, pH 7.0, and contained 0.05% NaN_3, 2 mM TCEP and 10% D_2O.

Two-dimensional TROSY spectra and the ^{15}N-separated nuclear Overhauser enhancement spectroscopy (NOESY)–HSQC and rotating frame nuclear Overhauser spectroscopy (ROESY)–HSQC spectra were acquired on a 700 MHz Varian spectrometer equipped with a room-temperature probe using standard pulse sequences with gradient coherence selection. The TROSY-selected ZZ-exchange experiment[35] was modified to include a lipid 'flipback' pulse and was acquired on a 800 MHz Bruker spectrometer equipped with a cryoprobe. ZZ-exchange spectra were acquired with mixing times of 20, 30, 40, 50, 80, 100, 130, 160 ms with 128 scans per increment and 128 complex points in the indirect dimension. Eighty per cent of the backbone resonances were assigned using a non-standard protocol combining standard triple resonance experiments (TROSY-HNCA, TROSY-HNCO, TROSY-HN(CO)CA) with amino-acid-specific labelling and ZZ-exchange data. NMR data were processed and analysed with NMRPipe[46], NMRView[47], Sparky[48] and IgorPro (Wavemetrics). All EmrE structure figures were created in PyMOL using Protein Data Bank 3B5D with the backbone rebuilt to render the cartoons. Full-page versions of the spectra in the main figures are included in the Supplementary Information.